Modulus Increase with Magnetic Field in Ferromagnetic Shape Memory Ni–Mn–Ga

LeAnn E. Faidley,[1] Marcelo J. Dapino,[1,*] Gregory N. Washington[1] and Thomas A. Lograsso[2]

[1]*Department of Mechanical Engineering, The Ohio State University Suite 255, 650 Ackerman Road, Columbus, OH 43202, USA*

[2]*Materials Engineering and Physics, Ames Laboratory Iowa State University, Ames, IA 50011, USA*

ABSTRACT: Ferromagnetic shape memory Ni–Mn–Ga has been shown to exhibit deformations of up to 9.5% when driven with quasistatic fields. This article is focused on the use of Ni–Mn–Ga as the active element in a dynamic transducer consisting of a solenoid and a low-reluctance, closed magnetic path. Despite the absence of a restoring force in this configuration, we have shown in prior studies recoverable compressible strains of $\lambda = -4100\,\mu\epsilon$, which are attributable to internal bias stresses built in the material during manufacture. In this study, we experimentally establish the presence of a modulus defect in $Ni_{50}Mn_{28.7}Ga_{21.3}$, whereby the elastic modulus increases as much as 255% upon increasing the applied magnetic field from zero to 380 kA/m DC. Experimental measurements are conducted under both mechanical and magnetic excitation, and analyzed in combination with vibratory models for the system. While in our experiments the attractive magnetic forces between the transducer poles may contribute to the total modulus increase, the presence of a modulus change associated with the Ni–Mn–Ga element is substantiated. Dynamic Ni–Mn–Ga transducers offer an attractive mechanism for electrical tuning of the modulus, with potential application in active vibration absorption problems.

Key Words: ferromagnetic shape memory alloys, Ni–Mn–Ga, solenoid transducer, dynamic transducer, elastic modulus defect.

INTRODUCTION

In 1996, Ullakko et al. (Ullakko et al., 1996) reported magnetic field-induced strains of up to 0.2% in stoichiometric Ni_2MnGa at 265 K. As work progressed with this material, it was found that off stoichiometric compositions exhibit larger strains of up to 6% at and above room temperature. The large strains and magnetic activation make Ni–Mn–Ga and other ferromagnetic shape memory alloys (FSMAs) attractive as actuator elements since materials exhibiting both large displacements and fast response times have been rare. These qualities make FSMAs promising for applications such as underwater communications, structural morphing concepts for aeronautics, and tunable stiffness resonators for noise and vibration control applications. Many of these applications require devices of compact size, high energy density, and broad frequency response, which are most easily achievable by solenoid-based actuators. However, results in the literature have been primarily focused on electromagnet-based transducers, which employ an orthogonal field-stress pair to generate reversible strains. In this study, we investigate the response of Ni–Mn–Ga rods driven in the collinear field-stress configuration encountered in solenoid transducers.

Ferromagnetic shape memory refers to either two mechanisms for magnetic field-induced strain. One mechanism lies in the structural transformation from austenite to martensite. This creates a strain due to the differing lattice parameters between the two phases, which is completely reversible upon removal of the field (James and Wuttig, 1998). The second mechanism involves the rearrangement of martensitic twin variants in response to magnetic fields and the creation of a strain due to the reorientation of non-cubic unit cells.

Over certain compositional ranges, the martensitic microstructure of Ni–Mn–Ga consists of a mixture of three martensitic variants, each with tetragonal lattice

*Author to whom correspondence should be addressed.
E-mail: dapino.1@osu.edu

1045-389X/06/02 0123–9 $10.00/0 DOI: 10.1177/1045389X06056061

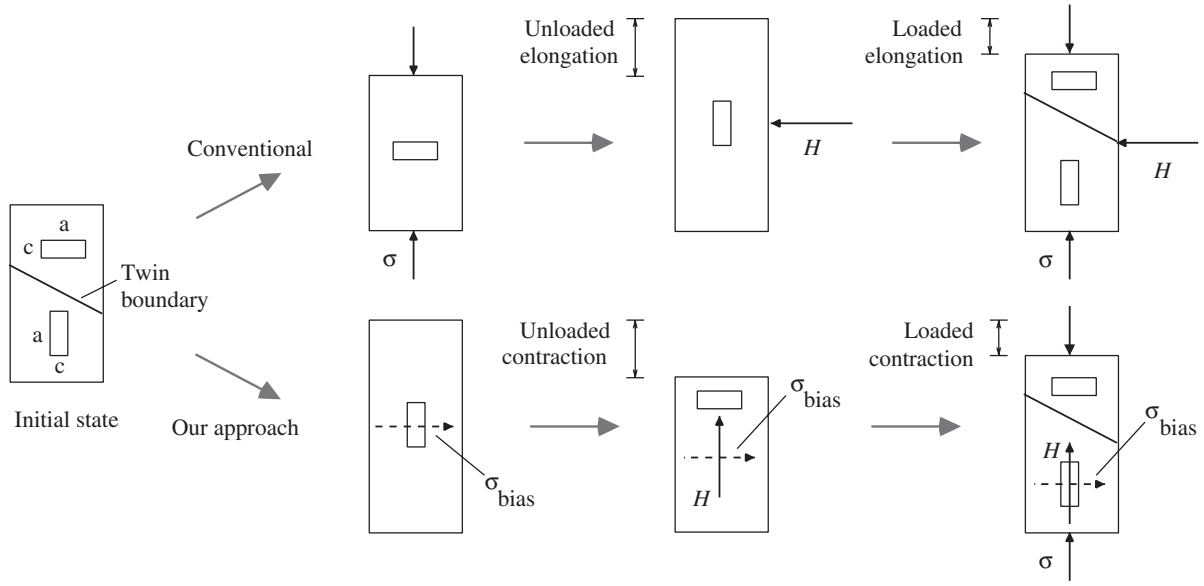

Figure 1. *Field-stress orientation for conventional and employed configuration.*

$a \times a \times c$ ($c < a$), in which adjacent variants are separated by a boundary known as a twin plane (Tickle et al., 1999). A two-dimensional representation of two variants in the initial state is shown on the left of Figure 1. Since the magnetic anisotropy of Ni–Mn–Ga is large compared with the energy required to change the volume fraction of each variant, the magnetization is rigidly attached to the shorter *c*-axis (Ullakko, 1996). When a magnetic field is applied, the variants with the *c*-axis aligned with the field are favored and grow at the expense of the other variants by way of twin boundary motion. Since the *c*-axis is the shorter of the crystallographic axes, a shortening of the bulk sample in the direction of the field occurs.

To achieve maximum deformations from Ni–Mn–Ga, preconditioning via a magnetic field or mechanical stress is commonly employed to induce a near-single variant with the short *c*-axis aligned with the load axis. Applying a large magnetic field of ≈5 kOe orthogonal to the load axis will induce a near-single variant with the *c*-axis aligned with the field, creating elongation strains of close to 6% for tetragonal five-layer Ni–Mn–Ga (Likhachev et al., 2001; Murray et al., 2001) and 9.5% for orthorhombic seven-layer Ni–Mn–Ga (Sozinov et al., 2002). However, since all twin variants have the same stability, there is no restoring force and the large strain is not recoverable without reconditioning of the sample (Murray et al., 2000). To achieve reversible strains, a mechanical compressive stress is applied orthogonal to the direction of the magnetic field, which favors variants with the *c*-axis aligned with the stress. Thus, a restoring force is applied, which leads to reversible strains (Likhachev et al., 2001). This process is displayed in the top portion of Figure 1 and denoted as the 'conventional' method. In practice, an electromagnet is needed to generate the magnetic field in this configuration.

This article is focused on the use of Ni–Mn–Ga in solenoid transducers rather than electromagnets. The former show promise of high energy density, compact size, and high frequency response up to 5 kHz (Faidley et al., 2003) because the closed magnetic circuit possible in solenoid designs facilitates the reduction of energy losses due to magnetic flux leakage. In solenoid transducers, the strain is measured along the direction of the applied magnetic field and the external mechanical load is parallel to this direction. This parallel drive configuration is shown at the bottom of Figure 1 and denoted as 'our approach'. Experimental measurements by Malla et al. (2003), which were independently verified as discussed by Faidley et al. (2004) show that large reversible compressive strains of at least $\lambda = -4100\,\mu\epsilon$ are achievable in this configuration despite the absence of an externally applied restoring force. It is hypothesized that during the rod manufacture, point defects and retained austenite are established, which impede the motion of the twin boundary and also create internal bias stresses that provide the restoring force necessary for reversible strain. Thus, as fields are applied the twin boundaries move so as to enlarge the favored variants. These boundaries are pinned in place as they encounter point defects and retained austenite, therefore limiting the possible bulk strain to values well below the 6% strains that are possible in alloys with nonexistent or relatively few pinning sites.

In addition to measured compressive strains of more than $\lambda = -4100\,\mu\epsilon$, we have measured significant elastic modulus increases of about 255% with increasing

bias field (Faidley et al., 2003, 2004). These increases are analogous to those seen in connection with the Delta-E effect in Terfenol-D (Clark, 1980; Flatau et al., 2000) and other magnetic materials (Chikazumi, 1964; Bozorth, 1993) and are extremely promising for applications in tunable vibration absorbers. A modulus decrease occurs in materials that include a mechanism for increasing the strain beyond the elastic strain (Cullity, 1972). This is called a modulus defect, of which the elastic modulus shift in magnetic materials caused by the dependence of strain on magnetization is a special case. As regards the Ni–Mn–Ga transducer, the additional strain is created by twin boundary motion, which is driven by an applied magnetic field. At saturation, this additional strain is minimized as no further twin boundary motion is possible. Thus, as the bias magnetic field is increased toward saturation, the modulus will increase toward the modulus for the material if the additional strain mechanisms did not exist.

EXPERIMENTS AND RESULTS

This experimental study is focused on the dynamic characterization of the elastic modulus of a single crystal alloy with composition $Ni_{50}Mn_{28.7}Ga_{21.3}$, which was prepared by the Bridgman method at Ames Laboratory. The single crystal ingot was oriented along the [100] direction, and a 0.248 in. (0.630 cm) diameter, 0.883 in. (2.243 cm) long rod was cut from the ingot using electrical discharge machining (EDM). The elastic modulus of the sample was determined using two different techniques where the field and stress were aligned collinearly. In the first technique, the sample was excited by a magnetic field applied in a solenoid transducer. The second technique involved exciting the sample mechanically using an eletrodynamic shaker.

Magnetic Excitation

EXPERIMENTAL APPARATUS

A broadband research transducer has been built to investigate the dynamic behavior of Ni–Mn–Ga samples driven in a collinear magnetic field-stress configuration (Malla, 2003; Malla et al., 2003). The transducer is shown in Figure 2 and consists of a water-cooled solenoid, pick-up coil, and magnetic steel components integrated to form a closed magnetic circuit. Materials employed in these components include stress-proof steel, 1018 steel, and pipe steel. The solenoid consists of 1350 turns of AWG 15 magnet wire and has a field rating of 167 G/A up to a maximum field of 8.1 kG. Distributed within the solenoid lies a coil of 0.25 in diameter copper tubing, which provides temperature control within $\pm 1^{\circ}$F

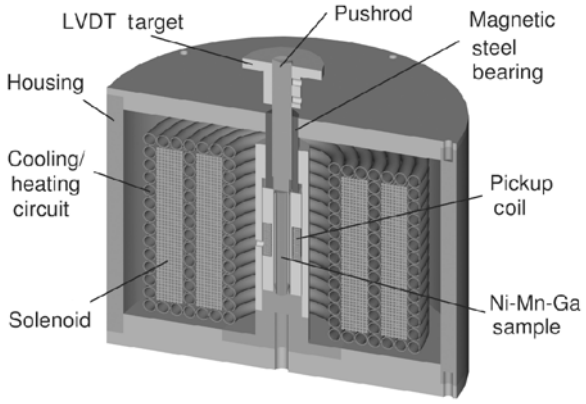

Figure 2. *Cross section of the broadband transducer employed in this study.*

by means of water flow at a rate of up to 6.35 L/min. The fact that the Ni–Mn–Ga rod is surrounded by a closed magnetic circuit ensures that demagnetization factors are negligible.

The solenoid was driven by two 4 kW Techron 7790 amplifiers arranged in series, with an overall voltage gain of 60 and a maximum output current of 56 A at the nominal solenoid resistance of 3.7 Ω. The magnetic induction was measured with a pickup coil made from AWG 33 insulated copper wire wound in two layers around an aluminum spool. Three Omega thermocouples were used to monitor the system temperature through a 10-channel Omega signal conditioner. The system was controlled by a SigLab 20-42 data acquisition system interfaced through a PC as illustrated in Figure 3.

The transducer was employed in these tests to measure the elastic modulus of a $Ni_{50}Mn_{28.7}Ga_{21.3}$ sample under various loads and bias magnetic fields. AC magnetic fields were applied using swept sine excitation between 100 and 5000 Hz, while the acceleration of the output pushrod and canister were measured by PCB 352C68 and U352C22 accelerometers mounted as shown in Figure 4. Two corresponding acceleration per current frequency response functions were measured and subsequently employed to determine the system resonances. The modulus dependence on load and bias field was determined by applying loads ranging from 40 to 750 g and bias fields ranging from 0 to 130 kA/m.

RESULTS

The measurements suggest that the transducer has numerous spectral components near the resonance frequency of the Ni–Mn–Ga element. To isolate the dynamic response due to the active element, the core material and mechanical load were changed and the auto spectral density of the canister and pushrod

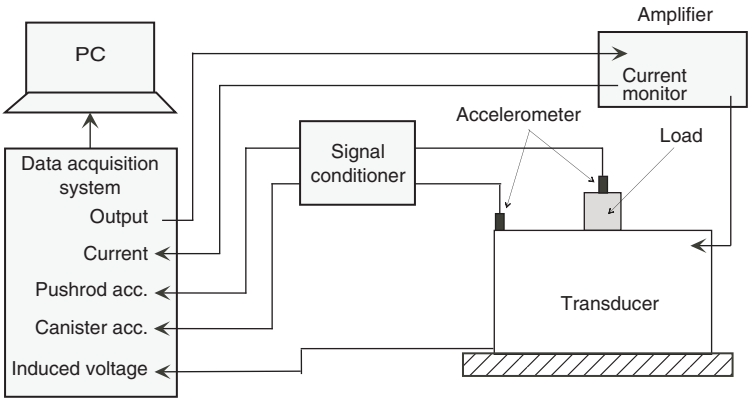

Figure 3. *Experimental setup used for dynamic testing of Ni–Mn–Ga.*

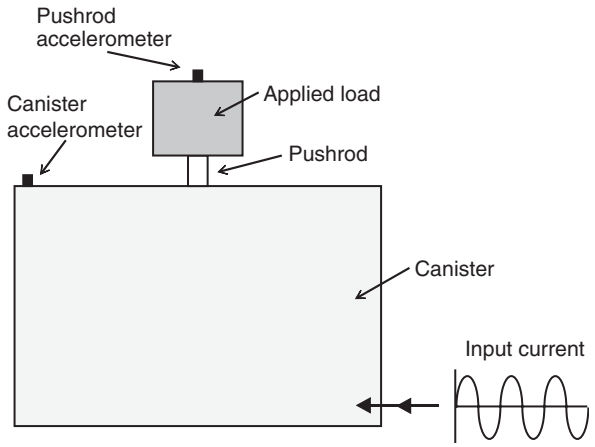

Figure 4. *Accelerometer placement during magnetic excitation modulus tests.*

acceleration signals were compared. The comparisons revealed that the resonance peak most closely linked to the sample is the peak located in the range between 500 and 1500 Hz (Faidley et al., 2003).

From a systems viewpoint, the transducer can be approximated as a one-degree-of-freedom (one DOF) second-order system. Mechanically, this system can thus be described by

$$m\ddot{x} + b\dot{x} + kx = F(t) \tag{1}$$

where m is the dynamic mass of the system, that is the sum of the applied mass and one-third the mass of the sample, end extensions, and pushrod; b is the intrinsic damping of the sample; k is the effective stiffness of the combination of Ni–Mn–Ga sample, end extensions, and pushrod; $x(t)$ is the displacement of the top of the sample; and $F(t)$ is the force on the sample generated from the application of a magnetic field. Observing that Ni–Mn–Ga responds to applied fields in a manner which is phenomenologically similar to giant magnetostrictive materials, an expression for $F(t)$ can be derived from the standard piezomagnetic equation

$$\epsilon = s^{\mathrm{H}} T + d^{\mathrm{T}} H, \tag{2}$$

which states that the strain ϵ is produced by a combination of stress T and applied magnetic field H. Parameter s^{H} is the compliance at constant field and d^{T} is the piezomagnetic coefficient at constant stress. Observing that $T = F/A$, where A is the cross-sectional area of the rod, and $H = nI$ where I is the current through a coil of n turns per length, the combination of Equations (1) and (2) yields the frequency response function acceleration per current,

$$\frac{\ddot{X}}{I}(j\omega) = \frac{-K\omega^2}{(k - m\omega^2) + jb\omega}, \tag{3}$$

which is of the standard second-order form with an extra double derivative made necessary by the fact that the acceleration is being measured rather than the displacement. Hence, the resonance frequency f of the system can be related to the mass and stiffness by

$$(2\pi f)^2 = \frac{k}{m}. \tag{4}$$

Figure 5 shows the resonance frequency measured for various mechanical loads under a fixed 1.1 kOe (86.2 kA/m) DC bias field and 82.7 Oe (6.6 kA/m) AC field amplitude. The close correlation between the relationship predicted by expression (4) and the experimental measurements shows the validity of the one DOF model over the region of interest.

Figures 6(a) and 7(a) show the frequency response functions of the output pushrod acceleration to input current for loads of 60 and 250 g, respectively, under various DC bias fields ranging from 0 to 1.6 kOe (0–129.3 kA/m). The shift in resonance frequency

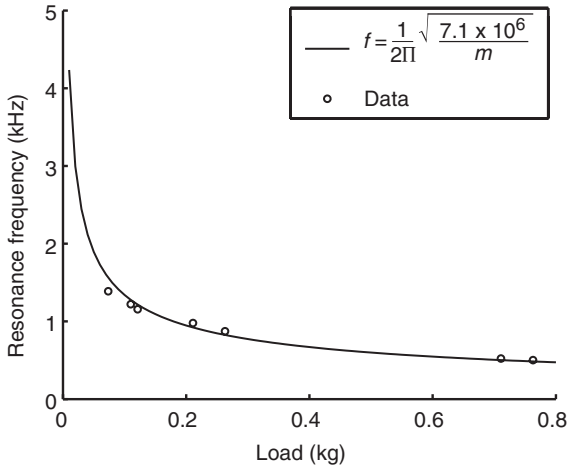

Figure 5. *Comparison of experimental and one DOF model results. The circles represent the resonance frequency f for various mechanical loads m, measured under a fixed 1.1 kOe (86.2 kA/m) DC bias field and 82.7 Oe (6.6 kA/m) ac field amplitude. The solid line was obtained from expression (4) with* $k = 7.1 \times 10^6$ *N/m.*

toward higher values indicates a stiffening of the Ni–Mn–Ga sample as the bias field is increased, which correlates to an increase in the elastic modulus of the sample. The modulus can be calculated by assuming a standard linear model for longitudinal rod vibrations

$$k = \frac{AE}{l}, \tag{5}$$

where A is the cross-sectional area of the rod, l is the length of the rod, and E is the elastic modulus. The modulus shift relative to zero field is defined by $(E - E_0)/E_0$ and is shown for different field levels in the top panel of Figures 6(b) and 7(b). In the bottom panel of Figures 6(b) and 7(b), the circles represent the magnitude of the frequency response function acceleration per current evaluated at resonance, while the diamonds represent the calculated values. The latter

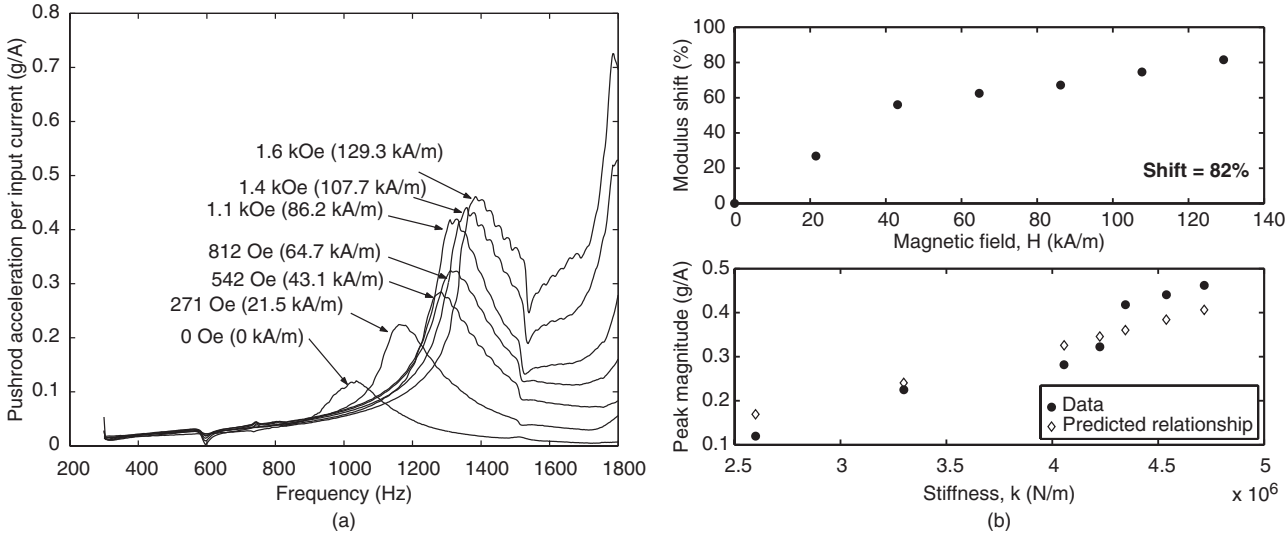

Figure 6. *Dynamic magnetic excitation of* $Ni_{50}Mn_{28.7}Ga_{21.3}$ *for various applied bias fields and 60-g load.*

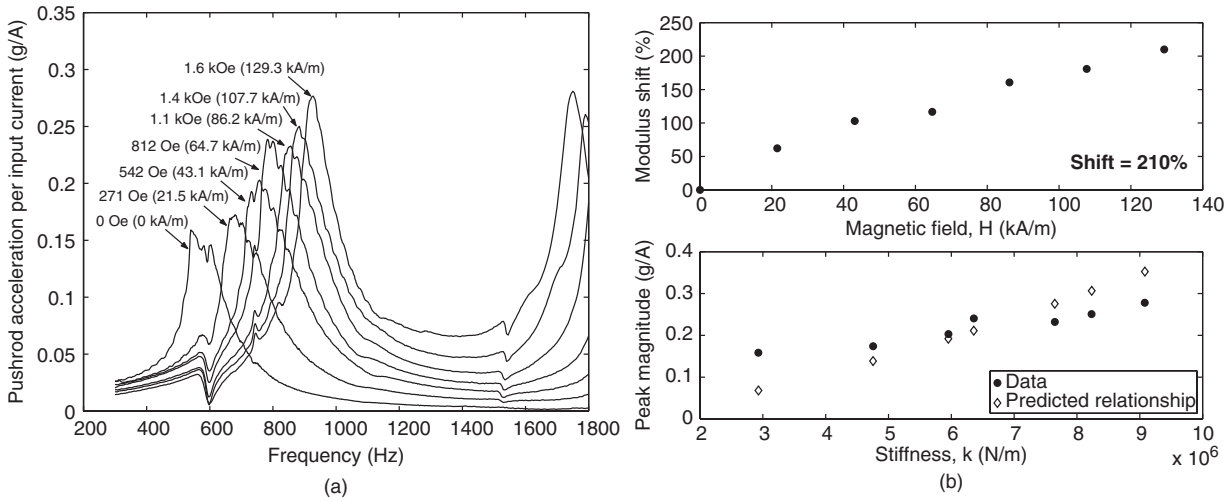

Figure 7. *Dynamic magnetic excitation of* $Ni_{50}Mn_{28.7}Ga_{21.3}$ *for various applied bias fields and 250-g load.*

are found by evaluating the magnitude of frequency response function (3) at the angular resonance frequency, $\omega_n = \sqrt{k/m}$,

$$\left|\frac{\ddot{X}}{I}(j\omega)\right|_{\omega=\omega_n} = \left|\frac{-K\omega_n^2}{(k - m\omega_n^2) + jb\omega_n}\right| = \frac{-K\omega_n^2}{b\omega_n} = \frac{-K\omega_n^2\sqrt{km}}{bk} = C\omega_n^2\sqrt{km},$$

where $C = -K/(bk)$ is a constant which needs to be determined from experimental data. The shift in elastic modulus for the 60-g case is monotonically increasing with a magnitude of 82% for a 1.5 kOe increase in bias field while the 250-g case has a total modulus shift of 210% with a 1.5 kOe increase in bias field.

Mechanical Excitation

EXPERIMENTAL APPARATUS

Magnetic forces exerted by the transducer steel components on the sample might affect the magnitude of the modulus increases measured using magnetic excitation. To investigate the significance of these forces, the Ni–Mn–Ga sample was isolated from the transducer using the apparatus shown in Figure 8. In this arrangement, the sample was mounted to the top of a Labworks ET-126 shaker driven by a Labworks PA-138 amplifier. The sample was placed in series with different combinations of Nd–Fe–B permanent magnets to create bias magnetic fields between 6.24 and 379.2 kA/m. Loads ranging from 0 to 250 g were mounted on top of the sample. The outputs from the system include the accelerations of the platform ($\ddot{x}_1$) and load ($\ddot{x}_2$), which were measured using PCB U353B16 and U353C22 accelerometers. The input is the displacement of the platform (x_0), which was controlled using a swept-sine excitation from 0.1 to 10 kHz provided by a SigLab 20-42 data acquisition system. The frequency response function relating the acceleration of the load to that of the platform was recorded for purposes of determining the resonance frequency and calculating the elastic modulus of the sample.

RESULTS

Test results for the 50-g external load case are shown in Figure 9. Since in this setup increasing the magnetic field in the sample also implies increasing the mass loading on the sample, the trends in modulus increase must be analyzed by considering the raw measurements in concert with a mechanical model for the system. To that end, the apparatus in Figure 8 can be

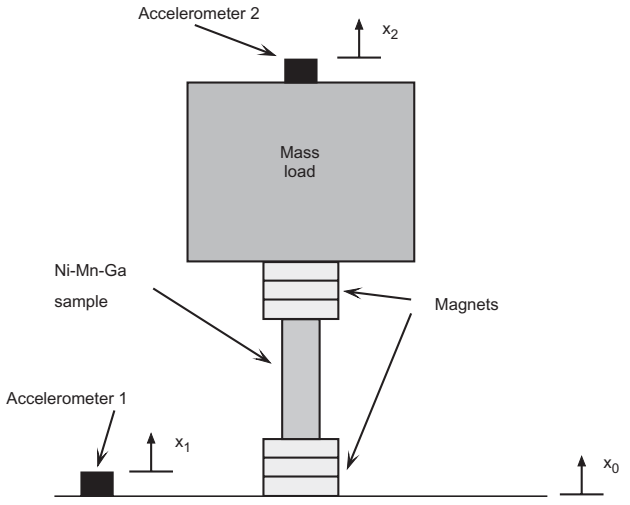

Figure 8. *Apparatus used for dynamic testing of the modulus shift through mechanical excitation with an electrodynamic shaker.*

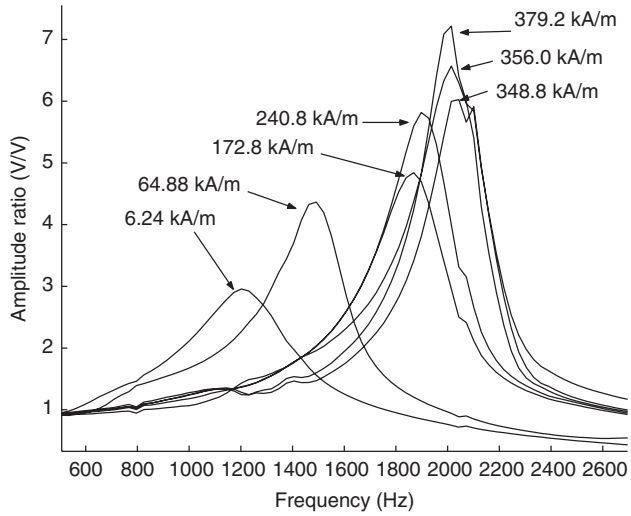

Figure 9. *Dynamic mechanical excitation of the Ni–Mn–Ga rod for various applied fields and a 50-g load.*

approximated as a one DOF system with base excitation. The system therefore has the following displacement transmissibility

$$\frac{X_2}{X_0}(j\omega) = \frac{\ddot{X}_2}{\ddot{X}_1}(j\omega) = \frac{jb\omega + k}{-m\omega^2 + jb\omega + k}. \qquad (6)$$

As in the magnetic excitation case, the resonance frequency of this system is given by Equation (4). This equation can be used in combination with Equation (5) to yield the elastic modulus of the sample taking into account the increase in load due to the addition of magnets on the top of the rod. The increase in elastic modulus relative to its value at zero field is plotted in Figure 10(a)–(d) for various mass loads. The lower panel of the individual plots shows the measured amplitude of the resonance peaks as well as the expected value based on the magnitude of the frequency response

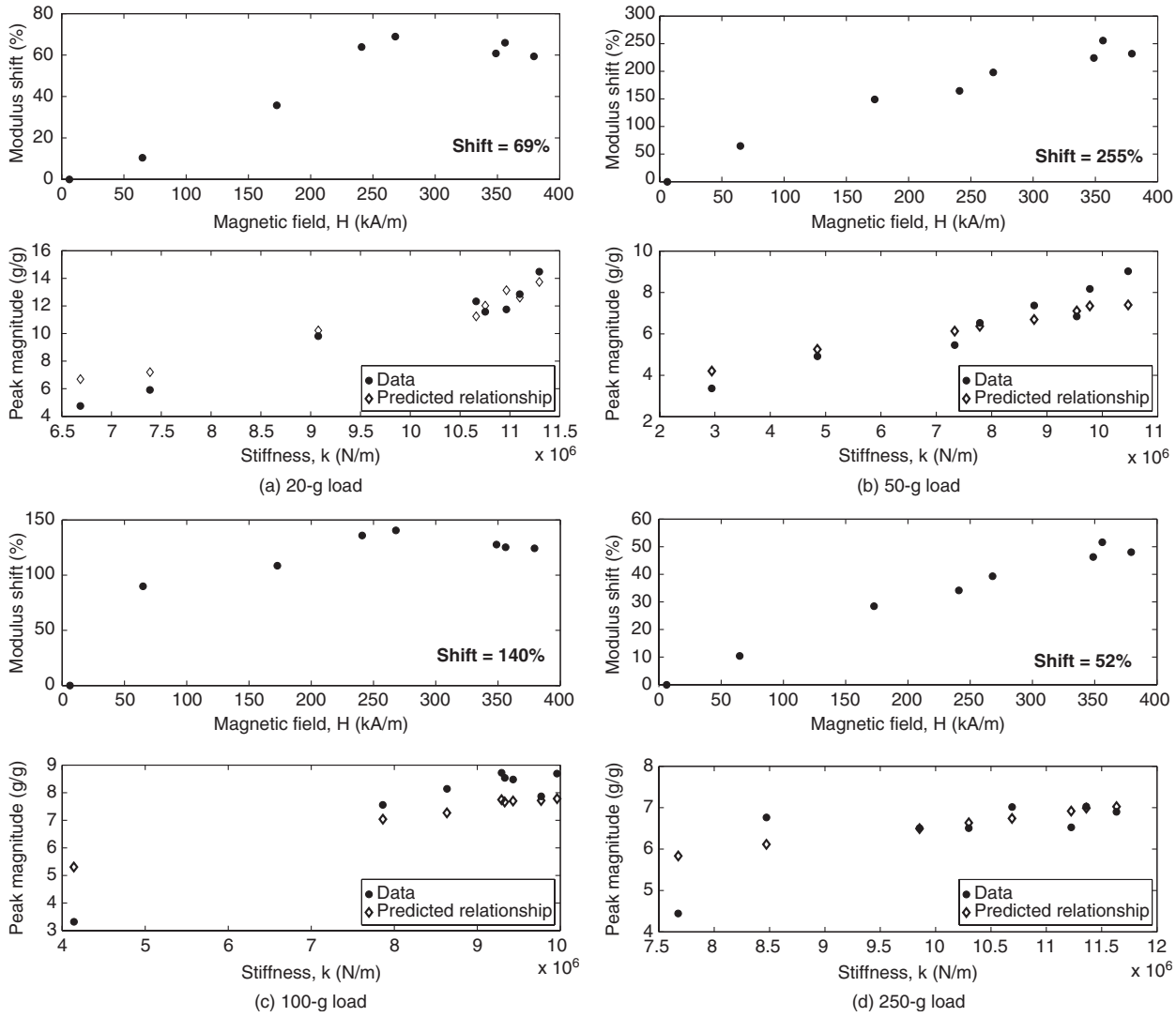

Figure 10. *Calculated elastic modulus increase and damping trend for various loads.*

function (6) evaluated at resonance, which in this case is proportional to $1 + C\sqrt{km}$. With a 373 kA/m increase in bias field, the overall increase in modulus varies between 52 and 255%. The dependence of the magnitude of the modulus variation on mass loading suggests the existence of an optimal load for obtaining maximum modulus variation.

DISCUSSION

Two facets of the observed modulus variation can be discussed based on the results presented in the previous section. The first is the large increase in modulus as the bias magnetic field is increased, which is quantified as being between 52 and 255% for various mass loads and excitation conditions. As a bias magnetic field is applied to the Ni–Mn–Ga sample, the variants with their shorter *c*-axis aligned with the field are favored and grow by way of twin boundary motion. This biases the initial magnetization toward the saturated state since in Ni–Mn–Ga the magnetization of the unit cell is fixed to the *c*-axis, and it also decreases the amount of strain that is possible from twin boundary motion. As discussed earlier, the amount of additional strain possible beyond the elastic strain is directly related to the decrease in elastic modulus from that of the material when only elastic strain is possible (Cullity, 1972). Thus, as the bias field is increased above zero, the modulus will also increase toward its saturation value consistent with the shifts of up to 255% observed in Figures 6, 7, and 10. The plots in Figure 10 also highlight the fact that the modulus varies less as the bias field approaches the level where the sample is saturated. The value of the field at which saturation begins to happen is significantly higher than the saturation field of the various steels used in the transducer, suggesting that the saturation of the modulus increase is due solely to the Ni–Mn–Ga sample. Should magnetic forces be

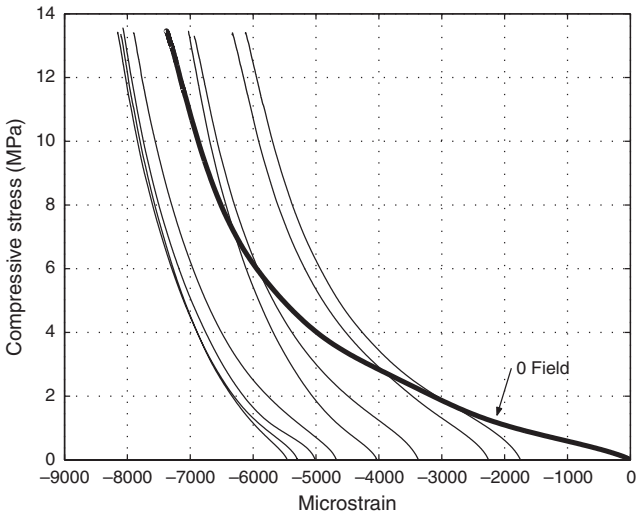

Figure 11. *Stress vs strain curves for the Ni–Mn–Ga sample employed in the study, for various bias fields.*

present, above magnetization saturation they would increase quadratically with increasing magnetic field since they depend on the square of the magnetic flux, which above magnetization saturation increases linearly with magnetization field. In other words, no saturation in the modulus would be present if magnetic forces were the only source of modulus change. While the presence of magnetic forces would result in an overestimation of the total modulus increase, the presence of a modulus increase in Ni–Mn–Ga between zero field and the modulus saturation field is established in this article.

The second aspect of the modulus variation that merits discussion is its nonlinear dependence on mass loading and the existence of an optimal mass load which yields the largest relative modulus increase. In the case of the magnetically excited system, the modulus shift increased from 82 to 210% as the load was increased from 20 to 250 g. For the mechanically excited system, there is an optimal load between 20 and 100 g, where there is a modulus change of more than 250%. This dependence on load is a consequence of the nonlinear nature of the stress–strain curve for the alloy employed in this study, shown in Figure 11. As the stress is increased, the material exhibits an initial purely elastic strain due to the compression of interatomic bonds, followed by strain due to twin boundary motion, which allows the large overall deformation of the material. The elastic modulus changes substantially through these two regions, which translates into a dependence of modulus on load. When a bias magnetic field is applied, it initializes the twin boundary strain prior to the elastic strain, changing the shape of the stress–strain curve and the relationship between stress and elastic modulus. This change in the stress dependence of the elastic modulus as the bias field is varied implies that the modulus shift with magnetic field will also show a related stress dependence. Similar dependencies are seen in other magnetic materials as discussed by Bozorth (1993).

Table 1. Summary of results for modulus shift with varying magnetic field.

Excitation	Load (g)	Bias field variation (kA/m)	Modulus shift (%)
Magnetic	60	0–130	82
Magnetic	250	0–130	210
Mechanical	20	0–380	69
Mechanical	50	0–380	255
Mechanical	100	0–380	140
Mechanical	250	0–380	52

CONCLUSIONS

Experimental results using both magnetic and mechanical excitation demonstrate the existence of an increase in modulus due to the application of a bias field to $Ni_{50}Mn_{28.7}Ga_{21.3}$ in a solenoid transducer configuration. The modulus change, which is summarized for various conditions in Table 1, qualitatively agrees with the increase in modulus that would be expected due to the additional strain possible because of magnetically induced twin boundary motion in Ni–Mn–Ga. The existence of these increases and their dependence on the external load agree with results reported in the literature for Terfenol-D and other more mildly magnetostrictive materials although the strain mechanisms are significantly different. The observed modulus increase of up to 255%, combined with the reversible strains of $\lambda = -4100\,\mu\epsilon$ that are achievable from this alloy composition when employed in a solenoid-based transducer, are very promising for numerous applications, especially for those involving tunable stiffness requirements, such as active vibration absorption or variable delay lines.

ACKNOWLEDGMENTS

The authors would like to acknowledge Aayush Malla for his assistance in aspects of the experimental testing. Funding for LEF is provided by the Ohio Space Grant Consortium. Funding for MJD was provided in part by the National Science Foundation under grant CMS-0409512.

REFERENCES

Bozorth, R.M. 1993. *Ferromagnetism*, IEEE Press, New York.

Chikazumi, S. 1964. *Physics of Magnetism*, John Wiley & Sons, New York.

Clark, A.E. 1980. Ferromagnetic Materials, In: Wohlfarth, E.P. (ed.), *Magnetostrictive Rare Earth-Fe_2 Compounds*, Chapter 7, pp. 531–589, North Holland Publishing Company, Amsterdam.

Cullity, R.D. 1972. *Introduction to Magnetic Materials*, Addison-Wesley Publishing Company, Reading, Massachusetts.

Faidley, L.E., Dapino, M.J., Washington, G.N. and Lograsso, T.A. 2003. "Dynamic Response in the Low-kHz Range and Delta-E Effect in Ferromagnetic Shape Memory Ni-Mn-Ga," In: *Proc. ASME/IMECE*, IMECE2003-43198.

Faidley, L.E., Dapino, M.J., Washington, G.N. and Lograsso, T.A. 2004. "Dynamic Behavior and Stiffness Tuning in Solenoid based Ni-Mn-Ga Transducers," In: *Proc. SPIE Smart Structures and Materials*, Vol. 5387, pp. 519–527.

Flatau, A.B., Dapino, M.J and Calkins, F.T. 2000. "High Bandwidth Tunability in a Smart Vibration Absorber," *Journal of Intelligent Material Systems and Structures*, 11(12):923–929.

James, R.D. and Wuttig, M. 1998. "Magnetostriction of Martensite," *Philosophical Magazine*, 77(5):1273–1299.

Likhachev, A.A., Sozinov, A. and Ullakko, K. 2001. "Influence of External Stress on the Reversibility of Magnetic-field-controlled Shape Memory Effect in Ni-Mn-Ga," In: *Proc. SPIE Smart Structures and Materials*, Vol. 4333, pp. 197–206.

Malla, A. 2003. "Effect of composition of the Magnetic and Elastic Properties of Shape Memory Ni-Mn-Ga," MS Thesis, The Ohio State University, Columbus, OH.

Malla, A., Dapino, M.J., Lograsso, T.A. and Schlagel, D. 2003. "Effect of Composition on the Magnetic and Elastic Properties of Shape-memory Ni-Mn-Ga," In: *Proc. SPIE Smart Structures and Materials 2003*, Vol. 5053, pp. 147–158.

Murray, S.J., Marioni, M., Allen, S.M., O'Handley, R.C. and Lograsso, T.A. 2000. "6% Magnetic-field-induced Strain by Twin-boundary Motion in Ferromagnetic Ni-Mn-Ga," *Applied Physics Letters*, 77(6):886–888.

Murray, S.J., Marioni, M., Tello, P.G., Allen, S.M. and O'Handley, R.C. 2001. "Giant Magnetic-field-induced Strain in Ni-Mn-Ga Crystals: Experimental Results and Modeling," *Journal of Magnetism and Magnetic Materials*, 226–230:945–947.

Sozinov, A., Likhachev, A.A., Lanska, N. and Ullakko, K. 2002. "Giant Magnetic-field-induced Strain in NiMnGa Seven-layered Martensitic Phase," *Applied Physics Letters*, 80(10):146–1748.

Tickle, R., James, R.D., Shield, T., Wuttig, M. and Kokorin, V.V. 1999. "Ferromagnetic Shape Memory in the NiMnGa System," *IEEE Transactions on Magnetics*, 35:4301–4310.

Ullakko, K. 1996. "Magnetically Controlled Shape Memory Alloys: A New Class of Actuator Materials," *Journal of Materials Engineering and Performance*, 5(3):405–409.

Ullakko, K., Huang, J.K., Kantner, C., O'Handley, R.C. and Kokorin, V.V. 1996. "Large Magnetic-field-induced Strains in Ni_2MnGa Single Crystals," *Applied Physics Letters*, 69(13): 1966–1968.